Phosphorescent Cocrystals Assembled by 1,4-Diiodotetrafluorobenzene and Fluorene and Its Heterocyclic Analogues Based on C−I⋯π Halogen Bonding

Hai Yue Gao, Xiao Ran Zhao, Hui Wang, Xue Pang, and Wei Jun Jin*

College of Chemistry, Beijing Normal University, Beijing 100875, P. R. China

S Supporting Information

ABSTRACT: Three phosphorescent cocrystals were prepared by 1,4-diiodotetrafluorobenzene and fluorene (cocrystal **1**) and its heterocyclic analogues, dibenzofuran (cocrystal **2**) and dibenzothiophene (cocrystal **3**), based on C−I⋯π halogen bonding, and C−H⋯π, C−H⋯I, or C−H⋯F hydrogen bonding as well as F⋯F and S⋯S contacts. They were well characterized by X-ray crystallography, infrared, Raman spectroscopy, and differential scanning calorimetry and thermogravimetric analysis. The calculated halogen and hydrogen bonding energies indicate that the synergistic double C−I⋯π in cocrystal **3** or $\pi \cdots_{XD}I_{HA} \cdots H$ patterns in cocrystal **2** really exist. 1,4-DITFB is a dual functional synthon: the cement to link luminescence molecules and a heavy atom

perturber to enhance phosphorescence of emitters by spin−orbital coupling. Three cocrystals phosphoresce distinctively with well defined vibrational bands at 496 (0−0) and 531 nm (max) for **1**, 496 (0−0) and 529 nm (max) for **2**, and 520 (0−0) and 564 nm (max) for **3**, respectively. All the decays obey a monoexponential law with lifetimes 0.34, 0.51, and 2.50 ms, respectively. The phosphorescence spectra of fluorene, dibenzofuran, or dibenzothiophene in cocrystals are largely red-shifted by approximately 50−90 nm with respect to the free monomer in β-cyclodextrin aqueous solution, indicating modulatory phosphorescence emission by the molecular structure of emitters *per se*, weak bonding, and the cocrystal environment.
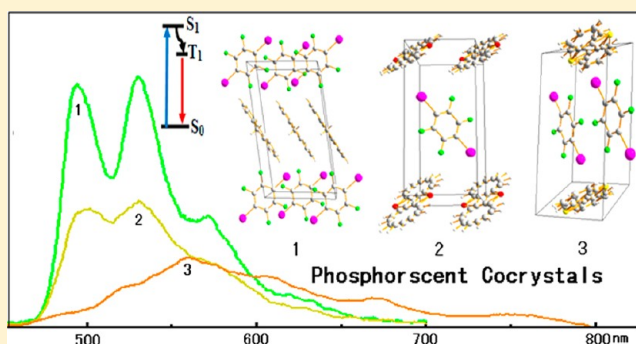
INTRODUCTION

Halogen bonding (XB) is a kind of intermolecular noncovalent interaction between the electron-deficient, polarizable halogen atom (Lewis acid, XB donor) and the electron-rich atom, anion, or π-electron system (Lewis base, XB acceptor).[1] In nature, XB is the attractive interaction between a region of positive electrostatic potential in a covalently bonded halogen atom and a negative site on an atom or group. Of course, electrostatic effects, polarization, charge transfer, and dispersion may all contribute to XB.[2−6] Because of its highly directional,[7] as well as fully hydrophobic, characteristics,[8] halogen bonding is developing into a common tool for the design and construction of supramolecular assemblies, and it is particularly becoming a popular means in the crystal engineering field.[9−14] Also, halogen bonding has become an important tool in molecular recognition,[15] design of drugs,[16] and exploration of biological interaction.[17,18]

1,4-DITFB is an excellent halogen bond donor because of the incorporation of strongly electron withdrawing groups attached to an I atom, resulting in the presence of a σ-hole acting as an XB donor site.[19] And frequently it is considered as a functional connective molecule in designing crystalline materials relevant to halogen bonding. It can also act as a heavy atom perturber in designing luminescent crystal materials, making the intersystem crossing rate k_{ISC} from both

S_1 to T_1 and T_1 to S_0 or S_1 faster; consequently, phosphorescence of the materials is enhanced.

Fluorene and its heterocyclic analogues, such as carbazole, dibenzofuran, and dibenzothiophene, *etc.*, have peculiar extensive π-conjugation electronic structure and highly emissive electron-conducting properties, which make them promising candidates for use in such diverse technologies as organic light-emitting diodes, photovoltaics, photorefractive electrolumines-cent devices, *etc.*[20−23] Generally, the purely organic materials emitting phosphorescence with long lifetime are very rare, and the few that are known are very inefficient emitters.[24] Moreover, crystallized organic luminescence materials can make the luminogens emitted in highly phosphorescently efficient at room temperature.[25] However, from the viewpoint of crystal engineering, the combination of different function-alized synthons in a cocrystal should be very important in improving the function of crystalline materials. So, the molecular cocrystals, in principle, could be made by 1,4-DITFB and fluorene and its heterocyclic analogues with predictable structures and improvable functions. The present work reports the crystallographic properties of three supra-

molecular cocrystals assembled by fluorene and its other two heterocyclic analogues with 1,4-DITFB, fluorine/1,4-DITFB (cocrystal **1**), dibenzofuran/1,4-DITFB (cocrystal **2**), and dibenzothiophene/1,4-DITFB (cocrystal **3**) based on a C–I···π halogen bond and C–H···π, C–H···I, and C–H···F hydrogen bonding, as well as F···F and S···S contacts. The differences of the three cocrystals in the crystal structures and phosphorescence behavior are also discussed. These phosphorescent organic cocrystals are easily synthesized by evaporation of organic solvent or precipitation in water phase, and it could be expected that they are useful in fabricating phosphorescent devices. Particularly, the S···S contact in cocrystal **3** should be conducive to designing new materials with both long lifetime luminescent and electron transport capacity.

■ EXPERIMENTAL SECTION

Fluorene (98%), iodobenzene (98%), and bromocyclohexane (98%) were purchased from Alfa Aesar Co. (WardHill, MA, USA). Dibenzofuran (98%) was purchased from J&K Scientific Ltd. Dibenzothiophene (98%) and 1,4-diiodotetrafluorobenzene (98%) were purchased from Sigma-Aldrich. Acetone and chloroform were purchased from Beijing Company of China National Medicals. β-Cyclodextrin (99%) was purchased from Yunan Yongguang Cyclodextrin Co. Ltd., Guangdong, China. All of the other starting materials were commercially available reagents of analytical grade and used without further purification. The chemical structures of fluorene and its heterocyclic analogues are shown in Scheme 1.

Scheme 1. Molecular Structures of Fluorene and Its Two Heterocyclic Analogues

Preparation of Cocrystals. *Cocrystal 1.* Fluorene and 1,4-DITFB in an equimolar ratio were dissolved in a 4:1 acetone/chloroform mixture solvent in a glass vial. The evaporation of the solvent at room temperature for three weeks yielded the colorless crystals. The product was isolated prior to full evaporation slowly of the solvent to guarantee the crystal purity. IR (ATR): ν_{max} 1466, 978, 945, 760, 747 cm^{-1}. Raman (solid): ν_{max} 158, 281, 499, 742, 786, 1018, 1233, 1477, 1611 cm^{-1}. Elemental analysis: (%): Calcd. for $C_{19}H_{10}F_4I_2$: C, 40.17; H, 1.77. Found: C, 40.13; H, 1.83.

Cocrystal 2. Dibenzofuran and 1,4-DITFB in an equimolar ratio were dissolved in 4:1 acetone/chloroform mixed solvent in a glass vial. The slow evaporation of the solvent at room temperature for 2 weeks yielded the colorless crystals. The product was isolated prior to full evaporation of the solvent to guarantee the crystal purity. IR (ATR): ν_{max} 1467, 1192, 978, 945, 839, 753, 721 cm^{-1}. Raman (solid): ν_{max}

157, 299, 499, 747, 1033, 1242, 1496, 1612 cm^{-1}. Elemental analysis: (%): Calcd. for $C_{18}H_8F_4I_2O$: C, 37.92; H, 1.41. Found: C, 37.93; H, 1.39.

Cocrystal 3. Dibenzothiophene and 1,4-DITFB in a 1:2 molar ratio were dissolved in 4:1 acetone/chloroform mixed solvent in a glass vial. The slow evaporation of the solvent at room temperature for 3 weeks yielded the colorless crystals. The product was isolated prior to full evaporation of the solvent to guarantee the crystal purity. IR (ATR): ν_{max} 1466, 981, 945, 761, 748 cm^{-1}. Raman (solid): ν_{max} 159, 283, 408, 500, 703, 1023, 1134, 1162, 1228, 1317, 1475, 1556, 1599 cm^{-1}. Elemental analysis: (%) Calcd. for $C_{24}H_8F_8I_4S$: C, 29.18; H, 0.82. Found: C, 29.31; H, 0.83.

Crystallography. XRD data of these cocrystals were collected at 293 K with a Bruker SMART APEX or Smart Apex II diffractometer using Mo Kα X-ray radiation (λ = 0.71073 Å) and a graphite monochromator. Empirical absorption corrections were applied using a multiscan method. The structures were resolved by a direct method and refined by full-matrix least-squares on F^2 using the SHELX program with anisotropic thermal parameters for all non-hydrogen atoms. H atoms were placed by calculation positions. The most relevant crystallographic data of the structure reported in this paper are shown in Table 1.

Table 1. Cocrystal Data and Structure Refinements

	cocrystal **1**	cocrystal **2**	cocrystal **3**
formula	$C_{19}H_{10}F_4I_2$	$C_{18}H_8F_4I_2O$	$C_{24}H_8F_8I_4S$
M_r	568.07	570. 04	987.96
cryst syst	monoclinic	triclinic	triclinic
space group	$C2$	$P\bar{1}$	$P\bar{1}$
a/Å	8.587(1)	5.425(2)	6.146(2)
b/Å	7.114(1)	5.769(1)	9.385(2)
c/Å	14.78(1)	13.91(1)	12.21(1)
α/deg	90	90.58(0)	74.32(1)
β/deg	99.20(1)	101.0(0)	89.80(0)
γ/deg	90	101.5 (1)	82.23(1)
V/Å^3	891.6(1)	418.3(2)	671.8(3)
Z	2	1	1
ρ_{calc}/(g cm^{-3})	2.116	2.263	2.442
μ(Mo KR)/mm^{-1}	3.564	3.803	4.785
$F(000)$	532	266	452
T/K	296(2)	150(2)	296(2)
hkl range	$-10 \leq h \leq 10$	$-6 \leq h \leq 4$	$-7 \leq h \leq 7$
	$-8 \leq k \leq 8$	$-6 \leq k \leq 6$	$-10 \leq k \leq 11$
	$-17 \leq l \leq 10$	$-16 \leq l \leq 15$	$-10 \leq l \leq 14$
measured refl	2026	2157	3215
unique refl/R_{int}	1379/0.0115	1487/0.0247	2399/0.0302
absorption correction	none	semiempirical from equivalent	semiempirical from equivalent
T_{min}/T_{max}	0.6544/0.4944	0.8326/0.4498	0.2636/0.2385
R1, wR2 [$I > 2\sigma(I)$]	0.0208, 0.0488	0.0535, 0.1328	0.0503, 0.1361
final R1, wR (F^2) values (all data)	0.0227, 0.0510	0.0575, 0.1367	0.0577, 0.1437
ρ_{fin}(max/min)/(e Å^{-3})	0.320/−0.562	4.640/−1.322	1.117/−1.272
goodness of fit on F^2	1.111	1.058	1.042

Spectroscopic Measurements. All phosphorescence spectra were recorded on a Cary Eclipse spectrophotometer (Varian) equipped with a flashed xenon lamp and with a 1 mm × 10 mm quartz cuvette at a 30/60° angle for the powder samples or ground cocrystals. The excitation wavelengths for three cocrystals were set at 280 nm, 330 nm, or 380 nm, respectively. Both excitation and emission bandpasses were set at the adaptive width (5/2.5 nm for **1**, 10/5 nm for **2**, and 20/10 nm for **3**). The delay time, gate time, and
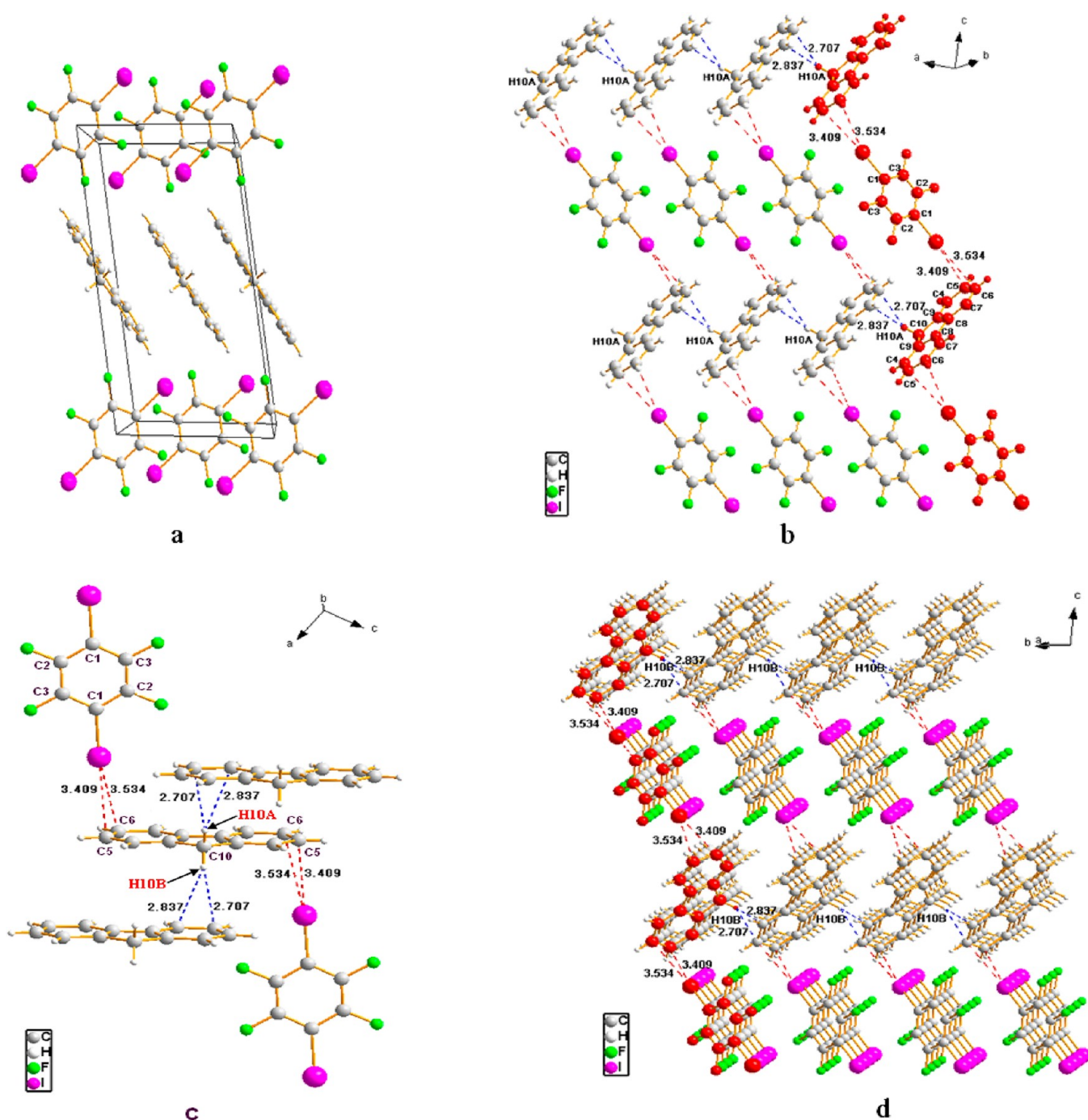
Figure 1. Crystal structures of cocrystal **1**. (a) Crystal cell unit. (b) Infinite chain stacking structures of cocrystal **1** formed by C−I···π and C−H···π. The red chain is a halogen bonding infinite chain. (c) Detailed diagram of bonding. (d) Packing diagram for cocrystal **1**. Color code: C, gray; H, white, F, green; I, purple. Part d was obtained by the horizontal flip of part b in the clockwise direction and extension of the fluorene to be adjacent another one by C−H10B···π bonding. (Two acidic H atoms in the same fluorene molecule are marked as H10A and H10B, respectively.)

total decay time were set as 0.1, 0.5, and 50 ms, respectively. The phosphorescence decay was measured under the same conditions.

A 10 mm × 10 mm quartz cuvette was used for β-CD aqueous systems by setting both ex/em slits at 20/20 nm; the delay time, gate time, and total decay time were set as 0.1, 0.5, and 50 ms, respectively. The excitation wavelengths were set at 260 nm (for fluorene), 290 nm (for dibenzofuran), and 280 nm (for dibenzothiophene), respectively.

Computational Methods. All calculations were carried out with the GAUSSIAN09[26,27] quantum chemistry package in the electronic ground state using dispersion-corrected density functional theory (DFT-D). The structures of all the monomers, dimers, and trimers were determined by XRD data and were used for a single point energy prediction by computational chemistry. The energies were obtained using B97D[28] with the 6-311++G** basis set for H, C, O, S, F atoms and 6-311G** for I atom. The interaction energy (DE) of each complex is calculated as the difference between the total energy of the complex and the sum of the total energies of the nucleophile and the acceptor. The basis set superposition error (BSSE) is also taken into account by means of the Boys−Bernardi counterpoise (CP) technique.

Differential Scanning Calorimetry and Thermogravimetric Analysis. Differential scanning calorimetry (DSC) was completed for the cocrystal powder samples at a rate of 10 °C/min using a differential scanning calorimeter (DSC 1, Mettler Toledo Co. Ltd.,

4379

dx.doi.org/10.1021/cg300515a | Cryst. Growth Des. 2012, 12, 4377−4387

Switzerland) under a nitrogen atmosphere. The range of temperature was 50−120 °C or 50−150 °C.

Thermogravimetric analysis (TGA) curves of the cocrystal powder samples were obtained using a thermogravimetric analyzer (TGA/DSC 1/1100, Mettler Toledo Co. Ltd., Switzerland) under a nitrogen atmosphere with a flow rate of 20 mL/min. Each sample was placed in a polytetrafluoroethylene crucible, and an empty one was used as reference. The range of temperature used was 50−300 °C with a heating rate of 10 °C/min to get the mass loss against heating temperature curves.

■ RESULTS AND DISCUSSION

Cocrystal Structures and Intermolecular Interactions. XRD analysis revealed a 1:1 stoichiometry for both **1** (fluorene/1,4-DITFB) and **2** (dibenzofuran/1,4-DITFB) and 1:2 for **3** (dibenzothiophene/1,4-DITFB), and their crystal structures are shown in Figures 1−3. Multiple interesting intermolecular interactions, including C−I···π halogen bonding, C−H···π, C−H···I, and C−H···F hydrogen bonding, and F···F and S···S interactions as well, are observed in these cocrystals, and the main bonding parameters are summarized in Table 2.

Table 2. Bonding Properties and Geometrical Parameters of Cocrystals

cocrystals	interactions	d/Å	θ/deg[a]	θ/deg
1	C−I···5C	3.409(10)	93.4(0)	171.3(0)
	C−I···6C	3.534(0)	88.2(1)	164.3(0)
	C−H···6C	2.707(1)	83.3(2)	142.4(0)
	C−H···7C	2.837(0)	78.3(0)	135.1(1)
2 A	C−I···6C	3.434(1)	85.5(0)	176.9(0)
	C−I···7C	3.517(1)	82.2(1)	156.8(1)
B	C−I···12C	3.546(1)	80.6(0)	166.8(1)
	C−I···13C	3.390(1)	86.8(3)	167.8(1)
	C−H··· I	3.080(0)	170.4(0)	170.4(1)
	C−H···F	2.506(1)	160.5(0)	160.5(0)
3 I	C−I···9C	3.502(1)	82.6(0)	168.8(0)
	C−I···10C	3.596(1)	76.1(0)	162.3(1)
	C−I···13C	3.556(1)	80.3(1)	172.6(0)
	C−I···14C	3.607(1)	77.8(0)	160.4(0)
II	C−I···7C	3.411(1)	85.4(8)	170.6(1)
	C−I···8C	3.655(2)	75.9(0)	148.3(1)
	C−I···12C	3.613(1)	77.5(6)	159.5(2)
	C−I···16C	3.487(1)	83.2(1)	170.4(0)
	C−I···17C	3.536(37)	80.6(11)	158.8(5)
	C−F···F−C	2.669(1)		167.0(1)
	S···S-plane	3.465(1)	89.1(1)	

[a]θ/deg means the angles C−I···molecular plane; A/B mean two sides of dibenzofuran in cocrystal **2**. Groups I and II in cocrystal **3**, cf. Figure 3b.

Cocrystal 1. As shown in Figure 1a, it crystallizes in the monoclinic space group C2 with four molecules in one unit cell. The infinite zigzag chain is constructed by C−I···π halogen bonding in an over-the-bond pattern of the I atom to the π-system (expressed in red in Figure 1b), and C−H···π between the H10A site at one fluorine and the π-system of another adjacent one connects the chains together (also the infinite fluorene molecular chains connected by the C−H···π can be regarded as the main chain). The resulting I···C distances are 3.409 and 3.534 Å with ∠C−I···C bonding angles of 171.3 and 164.3°, respectively. The H···C distances are 2.707 and 2.837 Å with ∠C−H···C bonding angles of 142.4 and 135.1°, respectively. The detail of the bonding is described in Figure

1c. All these distances are less than the sum of the van der Waals radii (Bondi radii, I 1.98 Å; Pauling radii, I 2.15 Å; half of the aromatic ring thickness, 1.85; Bondi radius, H 1.20 Å; Pauling radius, H 1.20 Å; Bondi radius, C 1.70 Å; Pauling radius, C 1.72 Å).[29,30] It can be seen that the halogen bonding is more apt to be linear than hydrogen bonding. As shown in Figure 1b, the fluorene acts as a halogen bonding acceptor interacting with the 1,4-DITFB molecule in a C−I···π pattern and a hydrogen bonding donor interacting with another adjacent fluorene molecule in a C−H···π pattern. So, the fluorene molecule has a dual bonding function in cocrystal **1**. There are no π···π stacks between 1,4-DITFBs or fluorenes. The 3D structure of cocrystal **1** (Figure 1d) is extended by the C−H10B···π bonding between fluorene and another adjacent one (Two acidic H atoms in the same fluorene molecule are marked as H10A and H10B, respectively).

Cocrystal 2. The nonresolvability of dibenzofuran molecules along its short axis orientation in the cocrystal results in a disorder structure, and there are two molecules in one cell unit, just one dibenzofuran and one 1,4-DITFB in 1:1 stoichiometry, as shown in Figure 2a. The cocrystal has a triclinic space group. The 3D structure of the cocrystal can be described as follows. First, the column-like infinite zigzag chain is constructed by C−I···π halogen bonding in an over-the-bond pattern of I atom to the π-system (expressed in blue in Figure 2b), and it also has C−H···I hydrogen bonding between the same I atom in the 1,4-DITFB molecule and one H atom of the dibenzofuran molecule in the adjacent chain to connect the chains together, as shown in Figure 2b. The resulting I···C distances are 3.434 and 3.517 Å, or 3.546 and 3.390 Å with ∠C−I···C bonding angles of 176.9 and 156.8°, or 166.8 and 167.8°, respectively. The side labeled with bonding length 3.517 and 3.434 Å is named as side A of the dibenzofuran plane. And the side labeled with bonding length 3.546 and 3.390 Å is named as side B. The H···I distance is 3.080 Å with ∠C−H···I bonding angle of 170.4°. If a dibenzofuran molecule is given a reversed orientation, the I···C or H···I distances and bonding angles in the sequentially resulting cocrystal structure are the same as the original ones. As shown in Figure 2c, the H atom on the lateral side of the dibenzofuran molecule contacts the F atom of 1,4-DITFB in the adjacent chain to form a C−H···F interaction, which should contribute to maintaining the stability of the 3D structure of the cocrystal. The shortest C−H···F contact is 2.506 Å with a bonding angle of 160.5°.

Cocrystal 3. It has a triclinic space group with one dibenzothiophene molecule and two 1,4-DITFB molecules in a 1:2 stoichiometry in one cell unit (Figure 3a). The dibenzothiophene molecule is nonresolvable along its short axis orientation, similar to the above dibenzofunan/1,4-DITFB or carbazole/1,4-DITFB cocrystals reported previously.[31] As shown in Figure 3b, the C−I···π bonding can be divided into two groups. In group I, the resulting I···C distances are 3.502, 3.596, 3.556, and 3.607 Å, with bonding angles of 168.8, 162.3, 172.6, and 160.4°, respectively. In group II, the bonding distances are 3.411, 3.655, 3.613, 3.487, and 3.536 Å, with bonding angles of 170.6, 148.3, 159.5, 170.4, and 158.8°, respectively. If a dibenzothiophene molecule is given a reversed orientation, the bonding distances and bonding angles in the sequentially resulting cocrystal structure are the same as the original ones. Just as in Figure 3b, the column-like infinite chain (expressed in yellow) is formed by a dibenzothiophene molecule as a nodal section with the alternative bonding of groups I and II.
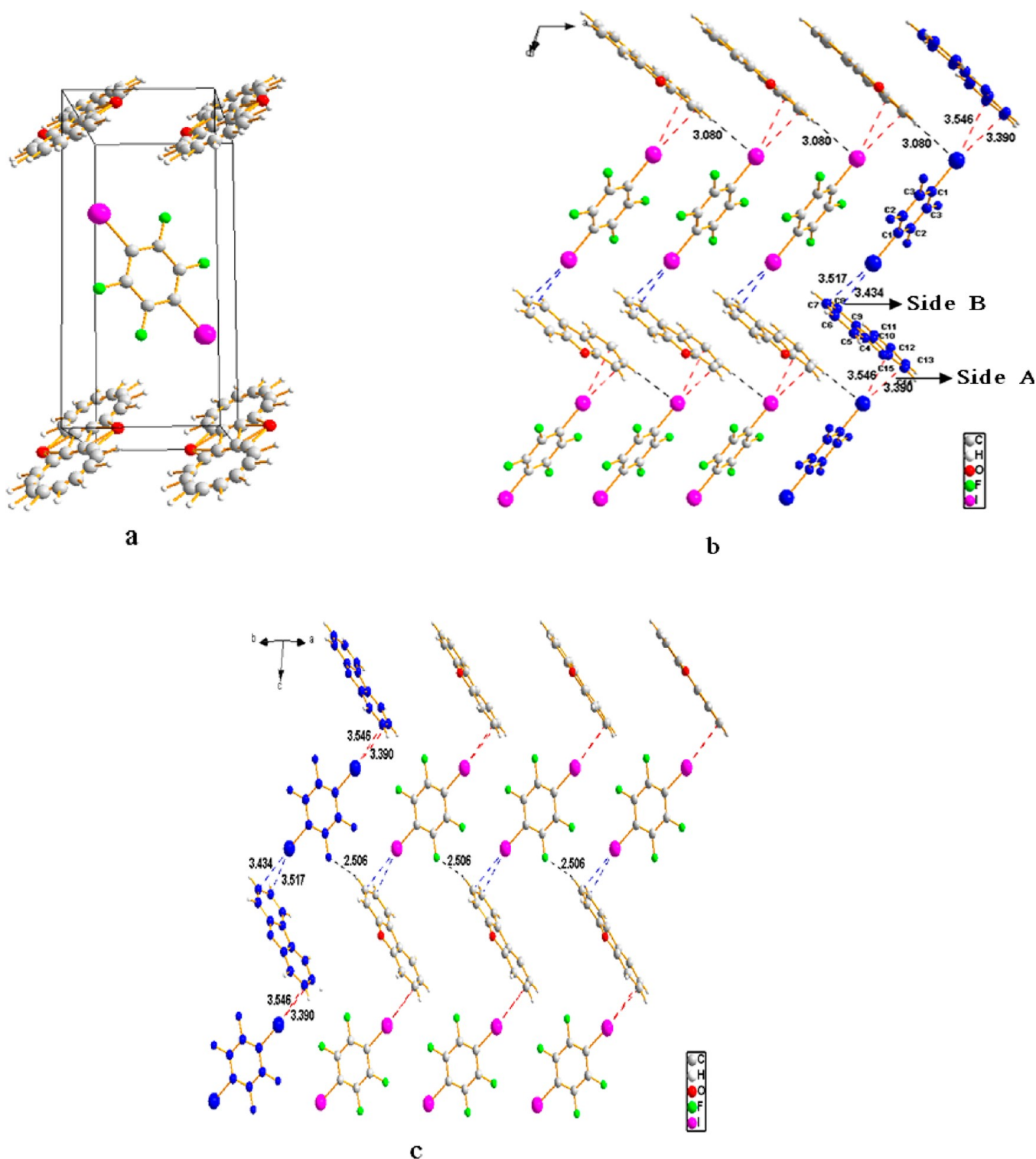
Figure 2. Crystal structures of cocrystal **2**. (a) Crystal cell unit. (b) Infinite main chain stacking structure of cocrystal **2** formed by C–I···π. The blue chain is a halogen bonding infinite chain. (c) Side packing diagram of part b. Color code: C, gray; F, green; I, purple; H, white; O, red.

For the 3D structure, the adjacent and parallel chains are connected mainly through S···S interactions and F···F contacts, as well as alternative bonding of groups II and I, as shown in Figure 3c. The shortest S···S contact is 3.465 Å with the angle of 89.1°, almost vertical to the dibenzothiophene plane. The S···S interactions should be interesting, just like the trans-annular conjugation of the σ-type observed in the phenathrene/1,4-DITFB cocrystal[32] or σ-, π-type or intermediate charge transfer.[33,34] Together with S···S interactions, the F···F contacts between 1,4-DITFB molecules with the distance of 2.669 Å (less than the sum of the van der Waals radii) and bonding angle of 167.0° also are necessary for the compact structure.

Calculations of Bonding Energies. The interaction units and their geometry parameters extracted from single cocrystal structure data for calculating energies are displayed in Figure 4, and the calculated bonding energies are listed in Table 3. The
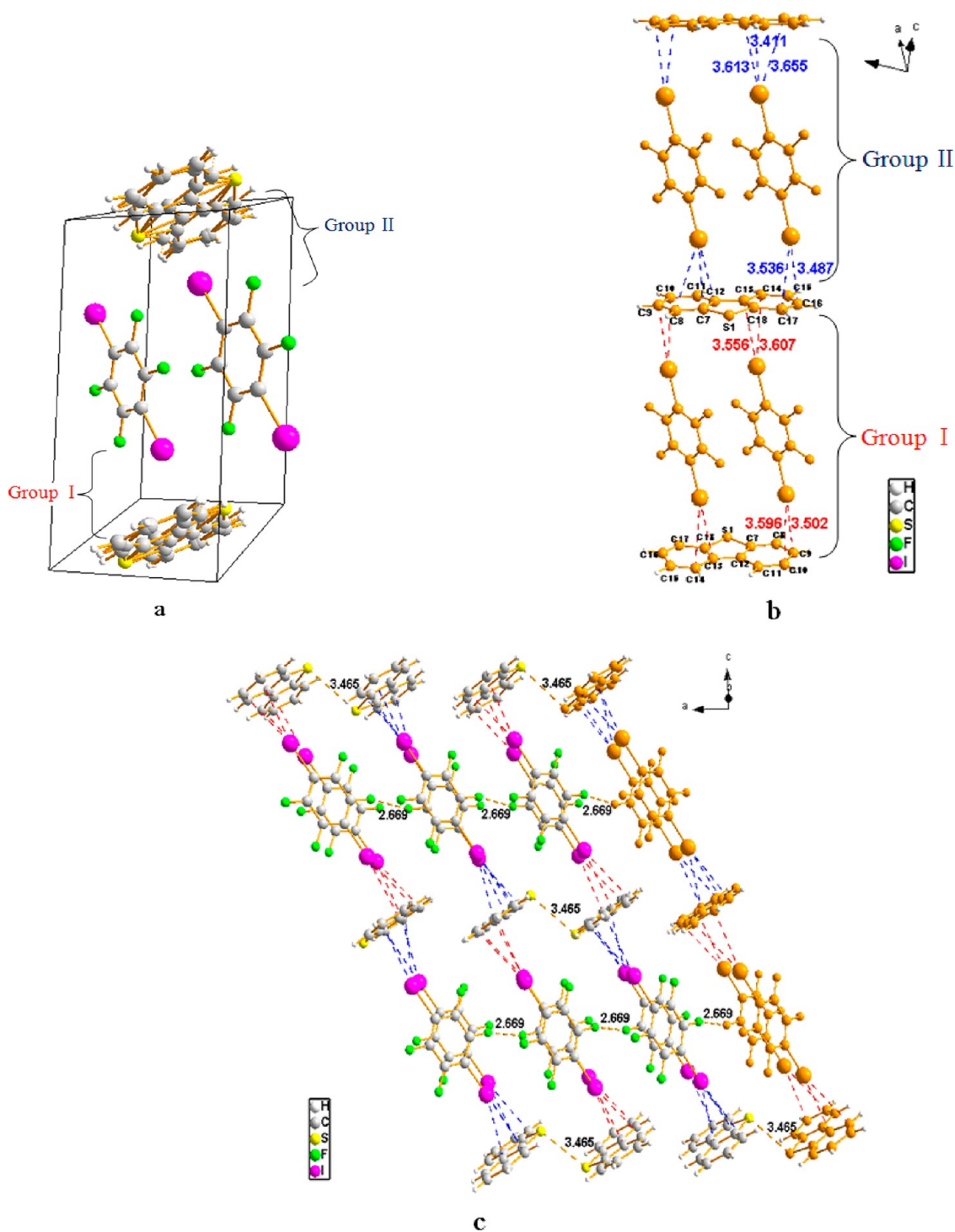
Figure 3. Crystal structures of cocrystal **3**. (a) Crystal cell unit. (b) Infinite main chain stacking structures of cocrystal **3** formed by C−I···π. The yellow chain is the halogen bonding infinite chain. (c) Packing diagram for cocrystal. Color code: C, gray; F, green; I, purple; H, white; S, yellow.

BSSE-corrected energy of C−H···π between adjacent fluorenes in cocrystal **1** is −26.2 kJ·mol^{-1}, greater than the C−I···π energies in all three cocrystals here, but very close to the C−I···π energy in the carbazole/1,4-DITFB cocrystal.[31] Among three cocrystals, the maximum C−I···π energy is −18.0 kJ·mol^{-1} in cocrystal **2**, which indicates an apparent synergistic effect of the π···$_{XD}$I$_{HA}$···H pattern compared with −11.3 kJ·mol^{-1} calculated per molar (D$_I$···A) unit (which does not exist individually) in cocrystal **3**. Next, the C−I···π energy is −33.9 kJ·mol^{-1} calculated per molar 2(D$_I$···A) unit in cocrystal

3, also indicating a synergy of double C−I···π bonding. The minimum C−I···π energy is −14.5 kJ·mol^{-1} in cocrystal **1**, maybe due to the result balanced by strong C−H···π bonding. All the C−I···π energies display the strong halogen bonding, being *ca.* 2−4 times greater than that in solution between 2-C$_3$F$_7$I or 1-C$_3$F$_7$I and toluene-d_8, where the calculated complexation energies are −6.4 or −5.4 kJ·mol^{-1}, respectively.[35]

The O or S atom in dibenzofuran or dibenzothiophene also could act as XB acceptor to form XB. But why not herein? Does
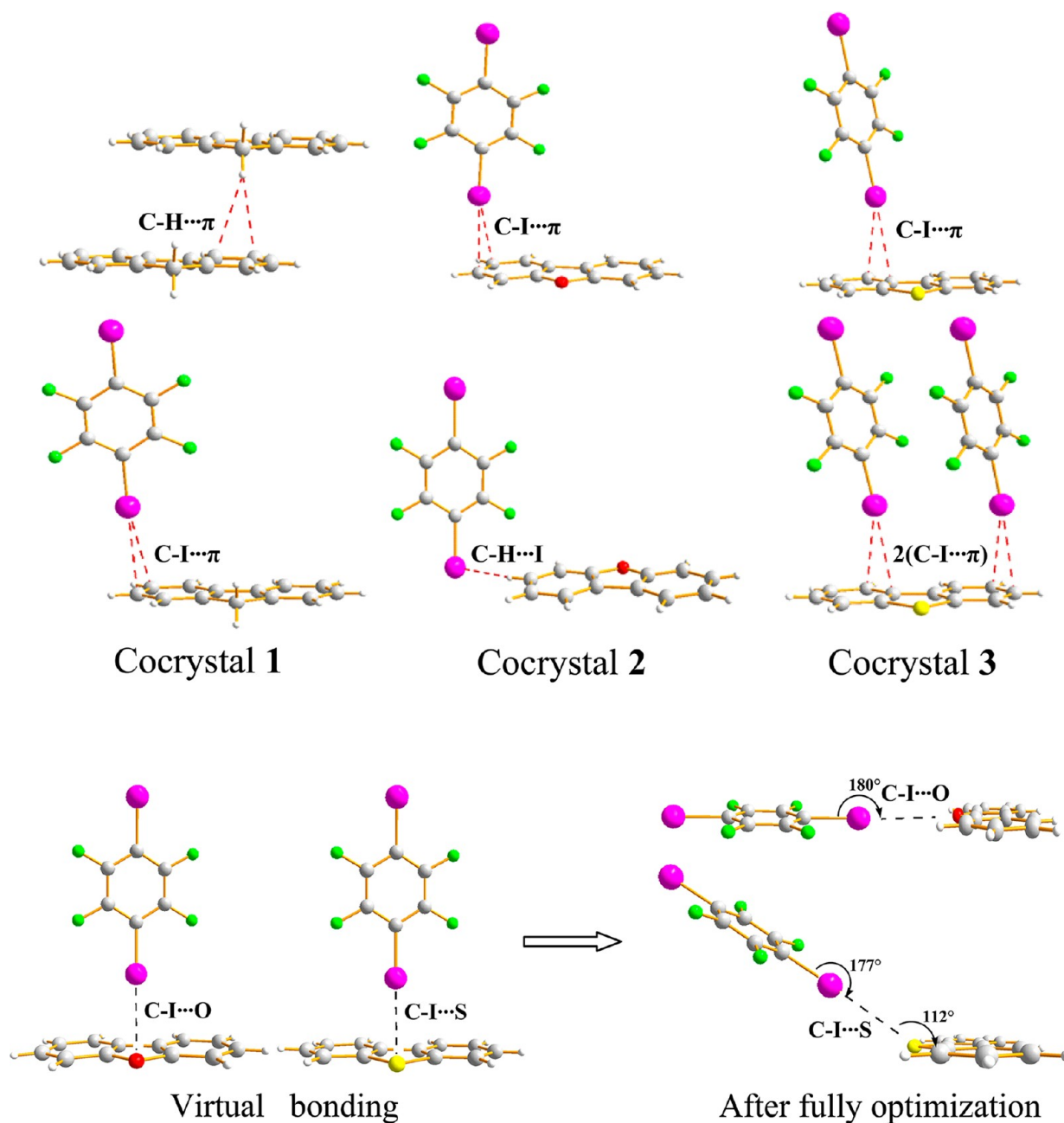
Figure 4. C−I···π halogen bonding, C−H···π or C−H···I hydrogen bonding units from single cocrystal structure data, and optimized C−I···O or C−I···S bonding units for calculation of energies (B97D with the 6-311++G** basis set for H, C, O, S, F atoms and 6-311G** for I atom).

it mean that the C−I···π halogen bond is easier to be formed than C−I···O or C−I···S in the corresponding system? The calculated binding energy of C−I···O or C−I···S based on the fully optimization structure of the C−I···O/S complex predicted in Figure 4 is −14.8 or −16.2 kJ·mol⁻¹, respectively. All of them are slightly less than that of C−I···π (−18.0 kJ·mol⁻¹ in cocrystal **2**) or half of 2(C−I···π) (−33.9 kJ·mol⁻¹ in cocrystal **3**). So, this may be the reason or one of the reasons why the C−I···O or C−I···S interaction does not occur in the prepared cocrystals. In addition, as shown in Figure 4, the C−I···O and C−I···S bonding angles are 180 and 177°, respectively. But, the angles of C−I···O and C−I···S are 180 and 112° with respect to the molecular plane. This means that the O atom in dibenzofuran keeps the approximate sp² hybrid state, while the S atom in dibenzothiophene keeps the sp³

hybrid state. So, the S−S contacts can occur in cocrystal **3** and dibenzothiophene has longer phosphorescence lifetime due to little contribution of lone pair electrons of the S atom to π-conjugation.

XRPD. For confirming the phase purity and homogeneity of the cocrystals, powder XRD patterns were carried out at room temperature. As shown in Figure S1 of the Supporting Information, the peak positions of experimental patterns (color curve) are in good agreement with curves simulated from single cocrystal XRD data (black curve), demonstrating a good phase purity of the bulk crystal products. The few discrepancies in intensity between simulated and experimental values may be the consequence of preferred orientations of the cocrystal powder samples.

Table 3. Calculated C−I⋯π Halogen Bonding, C−H⋯π or C−H⋯I Hydrogen Bonding, and Optimized C−I⋯O or C−I⋯S Bonding Unit Energies

cocrystal	bonding unit[a]	ΔE (kJ·mol^{-1})	ΔE^{CP} (kJ·mol^{-1})
1	D_H ⋯A (C−H⋯π)	−29.0	−26.2
	D_I⋯A (C−I⋯π)	−16.3	−14.5
2	D_I⋯A (C−I⋯π)	−20.1	−18.0
	D_H⋯A(I) (C−H⋯I)	−10.8	−9.25
	D_I⋯A (C−I⋯O)	−16.7	−14.8
3	D_I⋯A (C−I⋯π)	−13.4	−11.3
	$2D_I$⋯A 2(C−I⋯π)	−46.2	−33.9
	D_I⋯A (C−I⋯S)	−17.8	−16.2

[a]Note: the D_I stands for halogen bonding donor, 1,4-DITFB, or D_H stands for hydrogen bonding donor, fluorene or dibenzofuran. A stands for acceptor fluorene, dibenzofuran, and dibenzothiophene or I. ΔE: single point energy by B97D/6-311++G(d,p)/6-311(d,p). ΔE^{CP}: BSSE-corrected energies of ΔE.

ATR-IR and Raman Spectra. Interactions between the halogen bonding donor and acceptor in the cocrystals were investigated by FT-IR and Raman spectroscopy. As shown in Figure S2, FT-IR shows several significant differences of bound 1,4-DITFB compared with the free one. For free 1,4-DITFB, the fundamental band of a ring sextant ν_{C-C} stretch generally occurs in 1450−1600 cm^{-1} in FT-IR spectra. Herein it occurs at 1474 cm^{-1} (free) and 1466 or 1467 cm^{-1} (bound), respectively, red-shifted by 7−8 cm^{-1}.[36,37] The band at 158, 157, or 159 cm^{-1} in the Raman spectrum is due to a combined symmetrical C−I stretch and ring elongation and increases by 2−4 cm^{-1} compared with 155 cm^{-1} for free 1,4-DITFB.[38] All of them emphasize the presence of distinct interactions in the cocrystals and are in accord with a rule that the vibrational bands of the halogen-bonding donor in a halogen-bonded system exhibit a shift to lower wavenumber.

Differential Scanning Calorimetry Thermogram and Thermogravimetric Analysis. Figure 5 illustrates DSC thermogram and TGA curves of the three cocrystal powder samples. A sharp increase can be observed in the enthalpy relaxation as the cocrystals are heated to a temperature above the glass transition temperature. The areas of the endothermic peaks indicating melting points at Tp = 94.8 °C (cocrystal **1**), Tp = 99.2 °C (cocrystal **2**), and Tp = 85.9 °C (cocrystal **3**) in

the DSC scans give comparable enthalpies (ΔH) as −60.6, −70.9, and −55.6 J·g^{-1}, respectively. The other data of the cocrystals and raw materials are listed in Table S1. The starting decomposed temperature as well as the rate of thermal decomposition of the cocrystals can be obtained by TGA curves, as shown in Figure 5, and they are 94.0 °C/−99.2%, 113.3 °C/−96.7%, and 113.4 °C/−95.4%, respectively. The region is considered as the main decomposition step for these samples because the mass loss corresponds to 95.4% and 99.2% of the total mass loss.

Phosphorescence Spectra and Decays. It is well-known that fluorescence could be easily observed for fluorene and its heterocyclic analogues. However, the phosphorescence emission is difficult to be obtained due to the spin-forbidden $S_0−T_1$ and $S_1−T_1$ transitions. Introduction of a 1,4-DITFB molecule into the cocrystals would affect the luminescence characteristic of fluorene and its heterocyclic analogues. 1,4-DITFB plays two main roles in cocrystals: the cement to assemble fluorene and its heterocyclic analogue molecules to special crystalline materials, and the heavy atom perturber to induce phosphorescence emission by spin−orbital coupling. As shown in Figure 6 and Table 4, the cocrystal **1** emits strong phosphorescence. The phosphorescence emission spectrum goes from 490 to near 580 nm with well defined vibrational bands at 496 (0−0), 531 (max), 569, and 610 nm at the excitation wavelength of 280 nm. The phosphorescence of cocrystal **2** is obviously weaker with well defined vibrational bands at 496 (0−0), 529 (max), 572, and ∼597 nm at the excitation wavelength of 330 nm. The phosphorescence of cocrystal **3** is the weakest, with resolvable bands at 520 (0−0), 564 (max), 618, 669, and 748 nm at the excitation wavelength of 380 nm. The S⋯S interaction (assigned to π−π conjugation by σ-type overlap of π-orbitals of two different S atoms)[34] may make the gap between triplet and singlet ground states narrower and sequentially phosphorescence weaker compared with the case of cocrystal **1** or **2**. But it may provide the cocrystal additional function, such as electron transport.[39,40]

The cocrystals, as participation of microparticles with the same stoichiometry, also can be assembled very easily in aqueous solutions. The phosphorescence spectral and decay properties of the microparticles are the same with the cocrystals assembled by evaporation of organic solvent (*cf.* Figure S3).
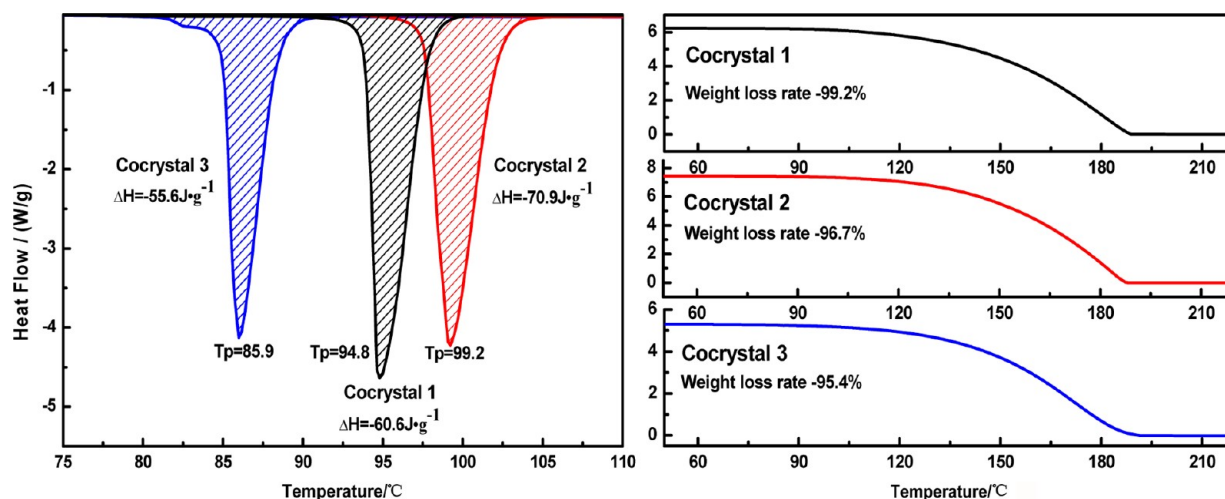
Figure 5. DSC (left) and TGA (right) curves of the three cocrystals.
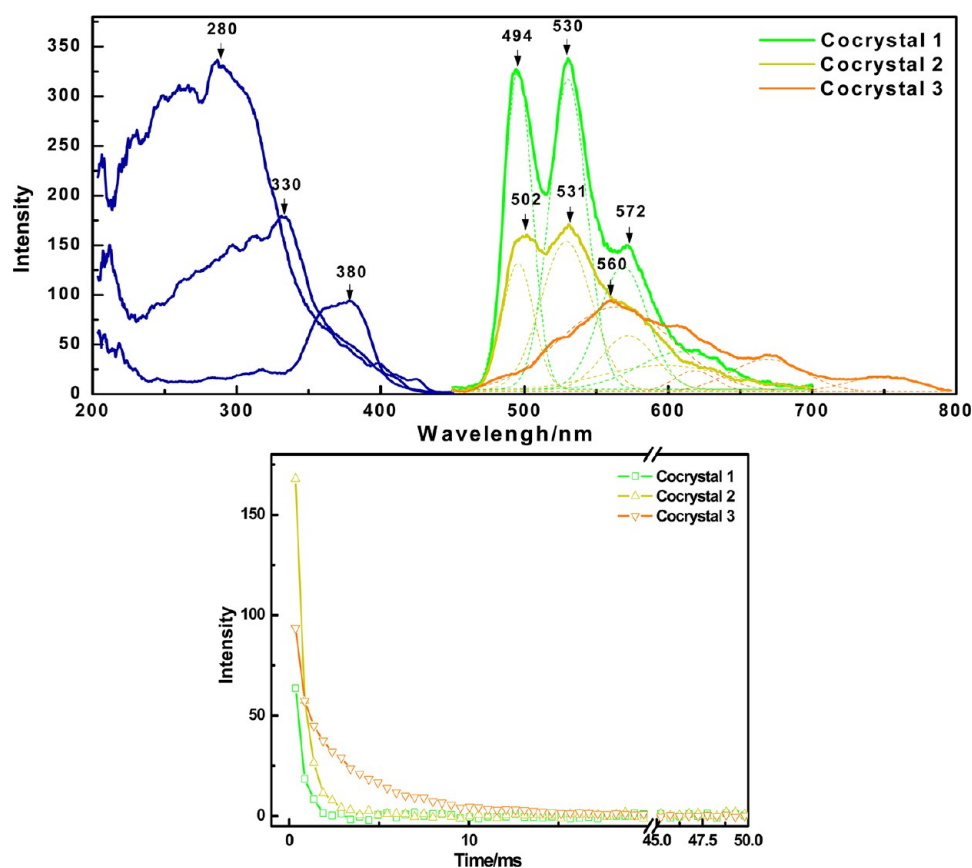
Figure 6. Phosphorescent excitation and emission spectra, and decay curves of cocrystals.

Table 4. Phosphorescent Characteristics of Fluorene, Dibenzofuran, or Dibenzothiophene

	excitation wavelengths/nm		emission wavelengths/nm		mean lifetime/ms	
	in cocrystals	in β-CD	in cocrystals	in β-CD	in cocrystals	in β-CD
fluorene	280	260	496 (0−0), 531 (max), 569, 610	~423 (0−0), 440 (max)	0.34	21.8/0.8[a]
dibenzofuran	330	290	496 (0−0), 529 (max), ~572, ~597	~429 (0−0), 450 (max)	0.51	27.4
dibenzothiophene	380	280	520 (0−0), 564 (max), 618, 669, 748	~436 (0−0), 467 (max)	2.50	25.7

[a]Note: the mean phosphorescent lifetime of fluorene is 0.8 ms using iodobenzene as heavy atom perturber in β-CD, while the lifetime of dibenzofuran or dibenzothiophene is not detectable under the same conditions, because of too weak a phosphorescent intensity.

The phosphorescence spectral positions of fluorene, dibenzofuran, and dibenzothiophene display no remarkable difference from those under similar conditions.[41,42] However, both the 0−0 and the maximum bands of fluorene, dibenzofuran, or dibenzothiophene in cocrystals are largely red-shifted by approximately 50−90 nm with respect to the free monomer emission in β-cyclodextrin (β-CD) aqueous solution induced by bromocyclohexane (Br-CH) or iodobenzene at room temperature, as shown in Figure 7, also compared to that on solid support induced by heavy metal ions.[43] In the β-CD cavity, fluorene, dibenzofuran, or dibenzothiophene is free, and the main force driving them into the cavity together with Br-CH to form a ternary inclusion complex is a hydrophobic or vdW interaction.[44] However, stronger chemically bonding interactions between molecules occur in cocrystals, as described in the structure section above, and these interactions should decrease the triplet state level of fluorene, dibenzofuran, or dibenzothiophene. The results signify that the phosphorescence emission can be modulated by not only the molecular structure of emitters but also the weak bonding and cocrystal environment.

The ex/em slits are 5/2.5 nm for cocrystal 1, 10/5 nm for cocrystal 2, and 20/10 nm for cocrystal 3. The positions of the vibrational bands labeled in Figure 6 refer to those before separation, and the vibration bands separated by assuming a Gaussian distribution of each band are listed in Table 4.

The phosphorescence decays were also studied, and the results are shown in Figure 6 and Table 4. The phosphorescence decays of three cocrystals obey a monoexponential law with the lifetime of 0.34 ms for cocrystal 1, 0.51 ms for cocrystal 2, and 2.50 ms for cocrystal 3, respectively. In suspension, microparticles of three cocrystals have the same phosphorescent lifetimes, while the mean phosphorescent lifetime of fluorene increases to 0.8 ms using iodobenzene as heavy atom perturber in β-CD. The phosphorescent lifetime of dibenzofuran or dibenzothiophene is not detectable under the same conditions, as the phosphorescent intensity is too weak. However, the mean phosphorescent lifetimes of fluorene, dibenzofuran, or dibenzothiophene using Br-CH as heavy atom perturber in β-CD are largely increased to more than 21.0 ms. The very similar phosphorescent lifetimes of three phosphorophores in β-CD using Br-CH as heavy atom perturber indicate
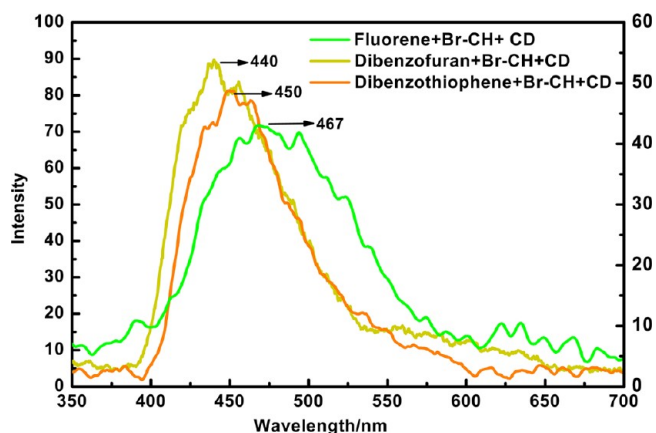
Figure 7. Phosphorescence emission spectra of fluorene and its heterocyclic analogues induced by bromocyclohexane (Br-CH) in β-CD aqueous solution. Conditions: [fluorine] and [dibenzofuran], 5.0×10^{-5} mol L^{-1}; [dibenzothiophene], 1.0×10^{-4} mol L^{-1}; [Br-CH], 2.0×10^{-5} mol L^{-1}; [β-CD], 8.0×10^{-3} mol L^{-1}. Excitation wavelength of 260 nm, 290 nm, and 280 nm, respectively, with the ex/em slits 20/20 nm. Also, replacement of Br-CH with iodobenzene as heavy atom perturber results in the same phosphorescent spectra but different lifetime.

that interaction between Br atom and guest molecule is limited to weak vdW force and physical spin–orbital coupling, while the interaction between I atom and phosphorophores in cocrystals is more complicated.

CONCLUSIONS

Halogen bonding provides a new strategy to assemble controllable functional cocrystals. Cocrystals **1**, **2**, and **3** are successfully constructed by 1,4-diiodotetrafluorobenzene and fluorene and its heterocyclic analogues based on C–I···π halogen bonding and/or C–H···π, C–H···I, F···F, and S···S interactions. The synergistic 2(C–I···π) in cocrystal **3** or π···$_{XD}$I$_{HA}$···H patterns in cocrystal **2** may provide a consideration in designing functional cocrystal engineering. Also, the S···S contact in cocrystal **3** should be conducive to designing new materials with both luminescent and electron transport capacity with its longer phosphorescence lifetime. The I atoms in the cocrystals act as a dual functional synthon: the cement and heavy atom perturber. As an expansion of functions besides the two above, the halogen bonding donors may provide other whole or localized cocrystal environments, such as polarity[19] and charity, to modulate the phosphorescence emission and decay. The halogen bonding donors also can act as "dilution agents" in cocrystals to protect the luminescence from quenching. In luminescent solid or film materials, the quenching phenomenon of luminogens caused by aggregation, such as excimers or exciplexes, is a thorny problem that had to be overcome. The crystallization induced phosphorescence (CIP) reported by Tang's group can resolve the problem to a certain degree.[45] However, the method seems efficient for the flexible phosphorescence molecules such as 4-bromobenzophenone, 4,4′-dibromobipheny, *etc.* For rigid and planar aromatic hydrocarbons, the method proposed herein to assemble phosphorescent cocrystals through halogen bonding and other assisting interactions may really provide a new strategy to overcome the quenching phenomenon caused by aggregation in the phosphorescent materials field.

ASSOCIATED CONTENT

Ⓢ Supporting Information

The experimental method and powder XRD, ATR-IR, and Raman spectra of the cocrystals or 1,4-DITFB; table of DSC and TGA data of the cocrystals or their raw materials; the experimental method, emission spectra, and decay curves of phosphorescence of the cocrystal suspended microparticles in water phase; and X-ray crystallographic information files (CIF) and checkCIF reports. This material is available free of charge via the Internet at http://pubs.acs.org.

AUTHOR INFORMATION

Corresponding Author

*E-mail: wjjin@bnu.edu.cn. Tel/Fax: (+86)10-58802146.

Notes

The authors declare no competing financial interest.

REFERENCES

(1) Metrangolo, P.; Neukirch, H.; Pilati, T.; Resnati, G. *Acc. Chem. Res.* **2005**, *38*, 386−395.

(2) Metrangolo, P.; Murray, J. S.; Pilati, T.; Politzer, P.; Resnati, G.; Terraneo, G. *CrystEngComm* **2011**, *13*, 6593−6596.

(3) Riley, K. E.; Hobza, P. *J. Chem. Theor. Comput.* **2008**, *4*, 232−242.

(4) Riley, K. E.; Murray, J. S.; Politzer, P.; Concha, M. C.; Hobza, P. *J. Chem. Theor. Comput.* **2009**, *5*, 155−163.

(5) Dikundwar, A. G.; Guru Row, T. N. *Cryst. Growth Des.* **2012**, *12*, 1713−1716.

(6) Webb, J. A.; Liu, P. H.; Malkina, O. L.; Goroff, N. S. *Angew. Chem., Int. Ed.* **2002**, *41*, 3011−3014.

(7) Clark, T.; Hennemann, M.; Murray, J. S.; Politzer, P. *J. Mol. Model.* **2007**, *13*, 291−296.

(8) Liang, W. J.; Wang, Y.; Feng, F.; Jin, W. J. *Anal. Chim. Acta* **2006**, *572*, 295−302.

(9) Nguyen, H. L.; Horton, P. N.; Hursthouse, M. B.; Legon, A. C.; Bruce, D. W. *J. Am. Chem. Soc.* **2004**, *126*, 16−17.

(10) Präsang, C.; Whitwood, A. C.; Bruce, D. W. *Chem. Commun.* **2008**, 2137−2139.

(11) Xu, J.; Liu, X.; Lin, T.; Huang, J.; He, C. *Macromolecules* **2005**, *38*, 3554−3557.

(12) Xu, J.; Liu, X.; Ng, J. K.-P.; Lin, T.; He, C. *J. Mater. Chem.* **2006**, *16*, 3540−3545.

(13) Yamamoto, H. M.; Kosaka, Y.; Maeda, R.; Yamaura, J.-I.; Nakao, A.; Nakamura, T.; Kato, R. *ACS Nano* **2008**, *2*, 143−155.

(14) Ji, B. M.; Wang, W. Z.; Deng, D. S.; Zhang, Y. *Cryst. Growth Des.* **2011**, *11*, 3622−3628.

(15) Caballero, A.; Zapata, Fabiola; White, N. G.; Costa, P. J.; Félix, Vltor; Beer, P. D. *Angew. Chem., Int. Ed.* **2012**, *51*, 1876−1880.

(16) Lu, Y. X.; Wang, Y.; Zhu, W. L. *Phys. Chem. Chem. Phys.* **2010**, *12*, 4543−4551.

(17) Voth, A. R.; Hays, F. A.; Ho, P. S. *Proc. Natl. Acad. Sci. U.S.A.* **2007**, *104*, 6188−6193.

(18) Parker, A. J.; Stewart, J.; Donald, K. J.; Parish, C. A. *J. Am. Chem. Soc.* **2012**, *134*, 5165−5172.

(19) Shen, Q. J.; Wei, H. Q.; Zou, W. Sh.; Sun, H. L.; Jin, W. J. *CrystEngComm* **2012**, *14*, 1010−1015.

(20) Bolton, O.; Lee, K.; Kim, H. J.; Lin, K. Y.; Kim, J. *Nat. Chem.* **2011**, *3*, 205−210.

(21) Dikundwar, A. G.; Dutta, G. K.; Guru Row, T. N.; Patil, S. *Cryst. Growth Des.* **2011**, *11*, 1615−1622.

(22) Vecchi, P. A.; Padmaperuma, A. B.; Qiao, H.; Sapochak, L. S.; Burrows, P. E. *Org. Lett.* **2006**, *8*, 4211−4214.

(23) Karim, Md. A.; Cho, Y. R.; Park, J. S.; Kim, S. C.; Kim, H. J.; Lee, J. W.; Gal, Y. S.; Jin, S. H. *Chem. Commun.* **2008**, 1929−1931.

(24) Bolton, O.; Lee, K.; Kim, H. J.; Lin, K. Y.; Kim, J. *Nat. Chem.* **2011**, *3*, 205−210.

(25) Yuan, W. Z.; Shen, X. Y.; Zhao, H.; Lam, J. W. Y.; Tang, L.; Lu, P.; Wang, C.; Liu, Y.; Wang, Z.; Zheng, Q.; Sun, J. Z.; Ma, Y.; Tang, B. Z. *J. Phys. Chem. C* **2010**, *114*, 6090−6099.

(26) Hauchecorne, D.; van der Veken, B. J.; Herrebout, W. A.; Hansen, P. E. *Chem. Phys.* **2011**, *381*, 5−10.

(27) Frisch, M. J.; Trucks, G. W.; Schlegel, H. B.; Scuseria, G. E.; Robb, M. A.; Cheeseman, J. R.; Scalmani, G.; Barone, V.; Mennucci, B.; Petersson, G. A.; Nakatsuji, H.; Caricato, M.; Li, X.; Hratchian, H. P.; Izmaylov, A. F.; Bloino, J.; Zheng, G.; Sonnenberg, J. L.; Hada, M.; Ehara, M.; Toyota, K.; Fukuda, R.; Hasegawa, J.; Ishida, M.; Nakajima, T.; Honda, Y.; Kitao, O.; Nakai, H.; Vreven, T.; Montgomery, J. A., Jr.; Peralta, J. E.; Ogliaro, F.; Bearpark, M.; Heyd, J. J.; Brothers, E.; Kudin, K. N.; Staroverov, V. N.; Kobayashi, R.; Normand, J.; Raghavachari, K.; Rendell, A.; Burant, J. C.; Iyengar, S. S.; Tomasi, J.; Cossi, M.; Rega, N.; Millam, J. M.; Klene, M.; Knox, J. E.; Cross, J. B.; Bakken, V.; Adamo, C.; Jaramillo, J.; Gomperts, R.; Stratmann, R. E.; Yazyev, O.; Austin, A. J.; Cammi, R.; Pomelli, C.; Ochterski, J. W.; Martin, R.; R. L., Morokuma, K.; Zakrzewski, V. G.; Voth, G. A.; Salvador, P.; Dannenberg, J. J.; Dapprich, S.; Daniels, A. D.; Farkas, O.; Foresman, J. B.; Ortiz, J. V.; Cioslowski, J.; and Fox, D. J. *GAUSSIAN09*; Gaussian, Inc.: Wallingford, CT, 2009.

(28) Grimme, S. *J. Comput. Chem.* **2006**, *27*, 1787−99.

(29) Bondi, A. *J. Phys. Chem.* **1964**, *68*, 441−451.

(30) Pauling, L. *The Nature of the Chemical Bond*; Cornell University Press: Ithaca, NY, 1945.

(31) Gao, H. Y.; Shen, Q. J.; Zhao, X, R.; Yan, X. Q.; Pang, X.; Jin, W. J. *J. Mater. Chem.* **2012**, *22*, 5336−5343.

(32) Shen, Q. J.; Pang, X.; Zhao, X, R.; Gao, H. Y.; Sun, H. L.; Jin, W. J. *CrystEngComm* **2012**, *14*, 5027−5034.

(33) Tang, X. D.; Liao, Y.; Gao, H. Z.; Geng, Y.; Su, Z. M. *J. Mater. Chem.* **2012**, *22*, 6907−6918.

(34) Huang, L.; Yu, D. Q. *Application of UV spectroscopy in organic chemistry (I)* (in Chinese); Science Press: Beijing, 1988.

(35) Hauchecorne, D.; van der Veken, B. J.; Herrebout, W. A.; Hansen, P. E. *Chem. Phys.* **2011**, *381*, 5−10.

(36) Liantonio, R.; Luzzati, S.; Metrangolo, P.; Pilati, T.; Resnati, G. *Tetrahedron* **2002**, *58*, 4023−4029.

(37) Messina, M. T.; Metrangolo, P.; Panzeri, W.; Pilati, T.; Resnati, G. *Tetrahedron* **2001**, *57*, 8543−8550.

(38) Graeme, R.; Hanson, P. J.; John, M.; Llew, R.; Aaron, S. M. *Chem.—Eur. J.* **2009**, *15*, 4156−4164.

(39) Huang, T. H.; Whang, W. T.; Shen, J. Y.; Wen, Y. Sh.; Lin, J. T.; Ke, T. H.; Chen, L. Y.; Wu, Ch. Ch. *Adv. Funct. Mater.* **2006**, *16*, 1449−1456.

(40) Wang, L.; Wu, Zh. Y.; Wong, W. Y.; Cheah, K. W.; Huang, H.; Chen, Ch. H. *Org. Electron.* **2011**, *12*, 595−601.

(41) Wang, X. H.; Tian, J. Q.; Kofron, W. G.; Lim, E. C. *J. Phys. Chem. A* **1999**, *103*, 1560−1565.

(42) Burress, C. N.; Bodine, M. I.; Elbjeirami, O.; Reibenspies, J. H.; Omary, M. A.; Gabba, F. P. *Inorg. Chem.* **2007**, *46*, 1388−1395.

(43) Vo-Dinh, T. *Room Temperature Phosphorimetry for Chemical Analysis [M]*; John Wiley & Sons: New York, 1984.

(44) Peng, Y. L.; Wang, Y. T.; Wang, Y.; Jin, W. J. *J. Photochem. Photobiol., A: Chem.* **2005**, *173*, 301−308.

(45) Luo, J.; Xie, Z.; Lam, J. W. Y.; Cheng, L.; Chen, H.; Qiu, C.; Kwok, H. S.; Zhan, X.; Liu, Y.; Zhu, D.; Tang, B. Z. *Chem. Commun.* **2001**, 1740−1741.